Practical Title: Measuring the Initial Mass Function (IMF)

Name: Hin Tsz Tseng (21065076)

Module Title: Star Formation & Steller Evolution

Submission Date: 13/4/2025

Abstract

The initial mass function (IMF) is crucial to the understanding of star formation and galaxy evolution. We present the measured α value of 2.25 ± 0.17 for 1 to 2 M_{Sun} main-sequence stars in the observed M35 cluster from the IMF plot, which aligns with the famous Salpeter value of 2.35 within the uncertainty range.

Researchers notice variations in the α value at two special masses for low-mass stars, 0.08 and 0.5 M_{Sun}, implying that the power law $\xi(m) \propto m^{-2.35}$ breaks for low-mass stars and that the Salpeter value of α does not apply to stars across all mass ranges. In the report, we explore how the different conditions in the star formation process contribute to the difference in α value between low and high-mass star formation regions.

Table of Contents

I. Introduction

The initial mass function (IMF) describes the initial mass distribution of stars born in regions of the star formation process. It sets the proportion of contributions different classes of stars make which tells us that low-mass stars dominate the stellar population on the galactic scale. Besides, the IMF sets the parameter to model the evolution of galaxies and chemical enrichment of the universe. Edwin Salpeter, an Austrian astronomer measured a well-known value of $\alpha = 2.35$ and informed us about the number of stars in the mass range of 1 to 2 M_{Sun} (Salpeter, 1955). His predictions align well with the α value for the stars with masses ranging from around 0.5 to 100 M_{Sun}.

Astronomers realise the difference in α value between low and high-mass star formation regions. This can be explained by the difference in the fragmentation process and the impact of feedback mechanisms on low and high-mass star formation regions.

In this report, we measure the α value for the M35 cluster from the main-sequence (MS) stars after correcting the presence of other irrelevant stars in the offset field and compare it to Salpeter's value. Our final result for α value is promising (2.25 ± 0.17), which is close to Salpeter's value within the error range.

II. Observations

Automated observations summary:

Objects	M35		M35 Offset Field	
Telescope used	CDK24			
Instrument	ASI Camera (1)			
Observation date	2025/02/05	2025/02/05	2025/02/05	2025/02/05
Observation time	22:28:29	22:34:01	22:41:56	22:50:54
Filter	V	B	V	B
Exposure time (s)	120	180	120	180
Binning	4 x 4			
E-gain	0.24665763974189758			
Airmass	1.17702635343		1.16313747432	
Plate-solved?	Yes			

Table 1: Summary table for M35 and its offset field.

Target parameters:

Objects	M35	M35 Offset Field
R.A. (J2000)	06h 09m 05s	05h 58m 07s
Dec (J2000)	+24° 20' 10"	+28° 41' 21"
Distance (pc)	830	
Age range (Myrs)	110 ~ 150	
A_V, A_B	0.81, 1.07	

Table 2: Parameter table for M35 and its offset field.

Refer the images for the cluster group and its offset field to the Appendix.

General comments:

I choose M35 for the practical since the cluster field is dense enough, and the stars from the field do not overlap that much with each other compared to M34 and M36.

The image quality is decent. The exposure time is chosen to optimise for $1M_{Sun}$ to $2M_{Sun}$ stars in M35 such that their flux will not saturate the peak pixel value. All the stars are well detected. Good SNR (V: 65.9, B: 35.1) and no fly-by objects in the images (e.g. satellites, planes).

III. Analysis & Results

A. Plot the colour-magnitude diagram: M_V vs. $(B - V)_0$

Given the apparent magnitudes in V-band (m_V) of the stars and the distance (d) in pc to the cluster, we use the distance-modulus relation (**Eq**. 1) to obtain the absolute magnitude in V-band (M_V) for each star in both clusters.

$$m - M = 5\log(d) - 5$$

$$\rightarrow M = m - 5\log(d) + 5 \ldots (1)$$

After correcting the star's apparent magnitudes for reddening and extinction in B and V-band using:

$$E(B-V) = A_B - A_V = (1.07) - (0.81) = 0.26 \ldots (2)$$

$$(B-V)_0 = (B-V) - E(B-V) = (B-V) - 0.26 \ldots (3)$$

, we can plot M_v against $(B\text{-}V)_0$. On the left plot of **Fig**. 1, we can see there is an obvious main sequence (MS) line on the colour-magnitude version of the Hertzsprung-Russel (HR) diagram for the M35. Then, we fit two straight lines enclosing the MS region for the M35 and its offset field respectively. Other irrelevant stars not residing on the MS line are removed for the following analysis part.

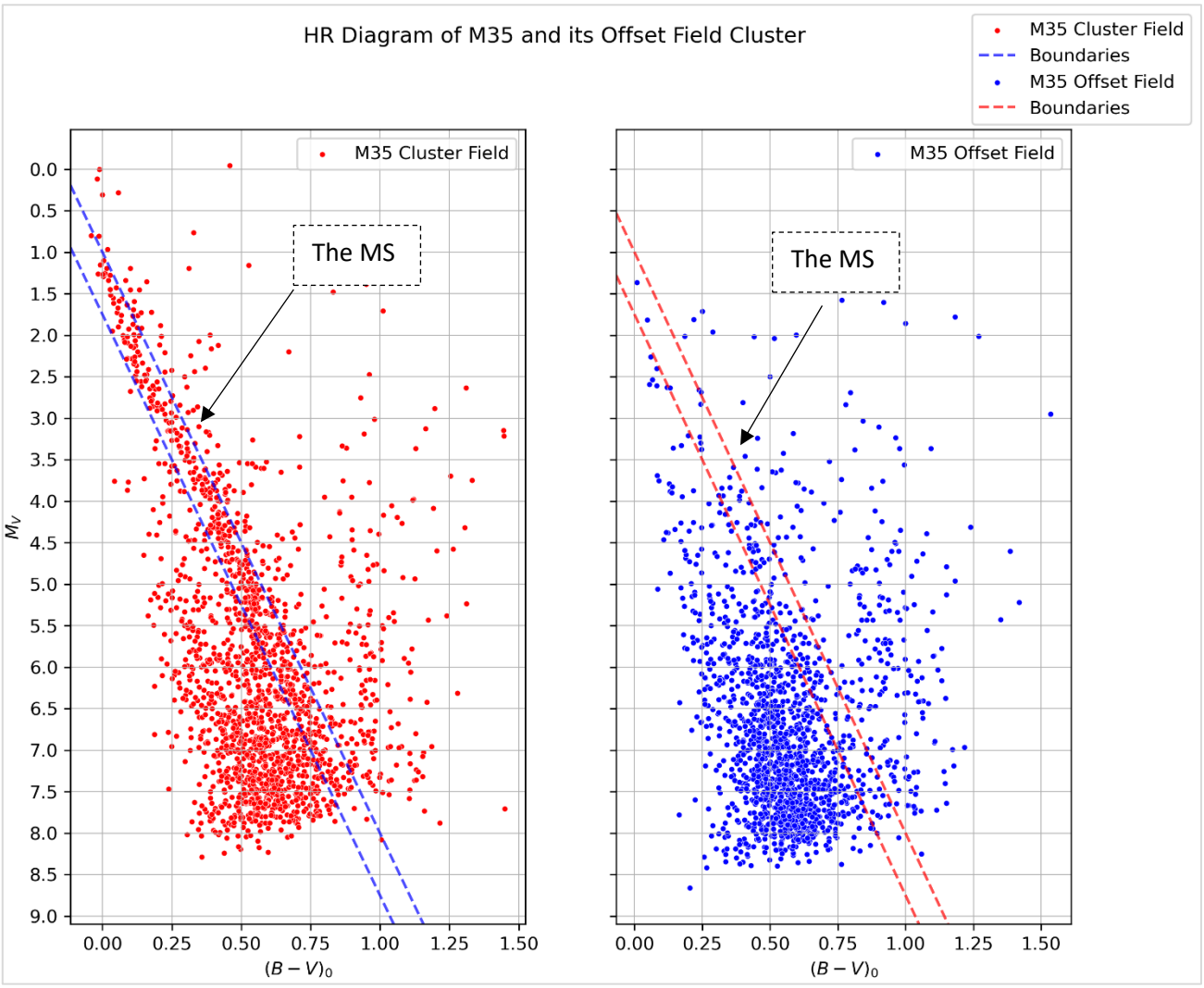

Figure 1: Colour-magnitude diagram of M35 and its offset field. The dashed lines show the boundaries that enclose the MS for both cluster fields.

B. Fit the M_{Sun} - M_V relation

To determine the star masses in terms of solar units (M_{Sun}) for M35 and its offset field, we implement a polynomial fit from the data provided, which takes M_V as the x values and masses in solar units as the y values. We include enough terms for the polynomial fitting to capture the delicate non-linear relationship between $M(M_{Sun})$ and M_V, while also not using too many terms to avoid overfitting.

After experimentation, we use 3 coefficients in the fitted polynomial line. It is a cubic equation with the following coefficients:

$$M(M_{Sun}) = -0.0086M_V^3 + 0.125M_V^2 - 0.811M_V + 2.981 \ldots (4)$$

If we flip the x-axis horizontally, we can see that the best fit (blue dashed) line depicts a slightly quadratic relation between M_{Sun} and M_V within the range from around 4.8 to 1.5 M_V. Then, we use this fitted line to predict the masses of the stars in terms of solar units with the calculated M_V in part (A).

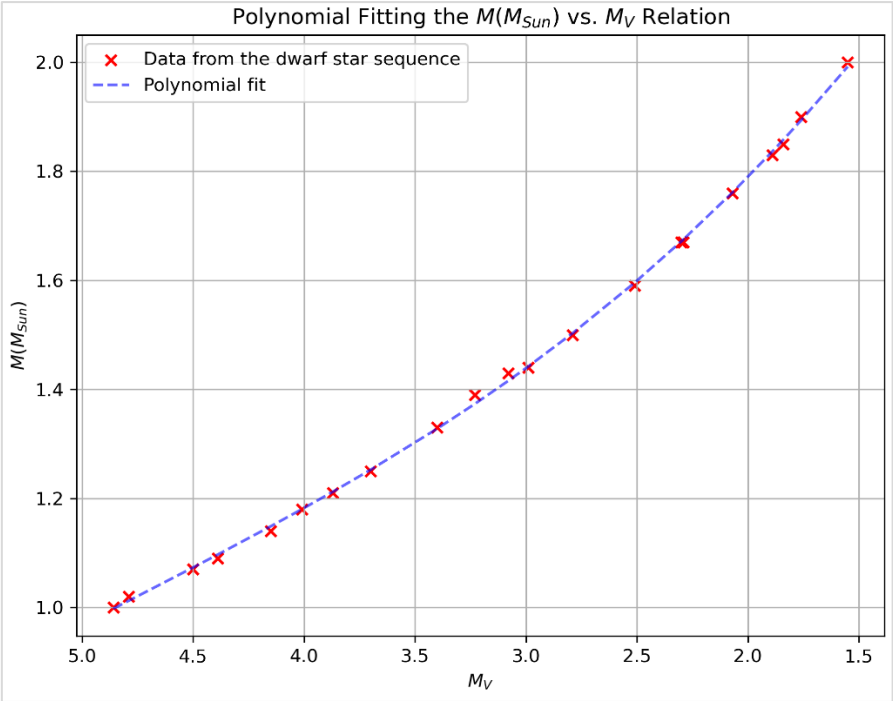

Figure 2: The relationship between $M(M_{Sun})$ and M_V. Note that the x-axis is flipped, starting with dimmer stars on the left to the brighter stars on the right.

C. Plot the IMF histogram

There are two ways to plot the IMF histogram, one is to plot $\xi(m)$ by setting up a series of bin masses (m) and directly obtain the value of α by fitting the slope. Another way is to plot log[$\xi(m)$] by setting up a series of log (m), by fitting the slope x and using the relation $x = \alpha - 1$, then we obtain α.

I choose to plot the first function, $\xi(m) \propto m^{-\alpha}$. The rule of thumb to choose the number of bins is to create as many bins as possible while ensuring that the maximum fractional error on $dn(cluster)$ for each bin is still less than 0.5. If we use too few bins, we cannot capture the overall pattern of the IMF. Too many bins will also result in a large fractional error. The data points will turn out to be inaccurate and noisy. After experimentation, I choose the bin size of 0.1 (i.e. 10 bins in total) for the MS stars ranging from 1 to 2 M_{Sun}.

Mass range for bins	1.00 ~ 1.10	1.10 ~ 1.20	1.20 ~ 1.30	1.30 ~ 1.40	1.40 ~ 1.50
Mid bin mass (m)	1.05	1.15	1.25	1.35	1.45
$log(m)$	0.0212	0.0607	0.0969	0.130	0.161
$dn(cluster\ field)$	44	46	34	24	25
$dn(offset\ field)$	17	15	5	3	1
$dn(cluster)$	27	31	29	21	24
$\delta[dn(cluster)] = \sqrt{dn(cluster) + dn(offset\ field)}$	±7.810	±7.810	±6.245	±5.196	±5.099
Fractional error on $dn(cluster)$	0.289	0.252	0.215	0.247	0.212
$\frac{dn}{dm}$, where dm = 0.1	270	310	290	210	240
$log\left(\frac{dn}{dm}\right)$	2.431	2.491	2.462	2.322	2.380
$\delta\ log\left(\frac{dn}{dm}\right)$	±0.126	±0.109	±0.094	±0.107	±0.092

1.50 ~ 1.60	1.60 ~ 1.70	1.70 ~ 1.80	1.80 ~ 1.90	1.90 ~ 2.00
1.55	1.65	1.75	1.85	1.95
0.190	0.217	0.243	0.267	0.290
17	20	19	11	11
2	0	0	1	0
15	20	19	10	11
±4.359	±4.472	±4.359	±3.464	±3.317
0.291	0.224	0.229	0.346	0.302
150	200	190	100	110
2.176	2.301	2.279	2.000	2.041
±0.126	±0.097	±0.100	±0.150	±0.131

Table 3: Summary table of data for plotting ξ (m), where ξ (m) $\propto m^{-\alpha}$.

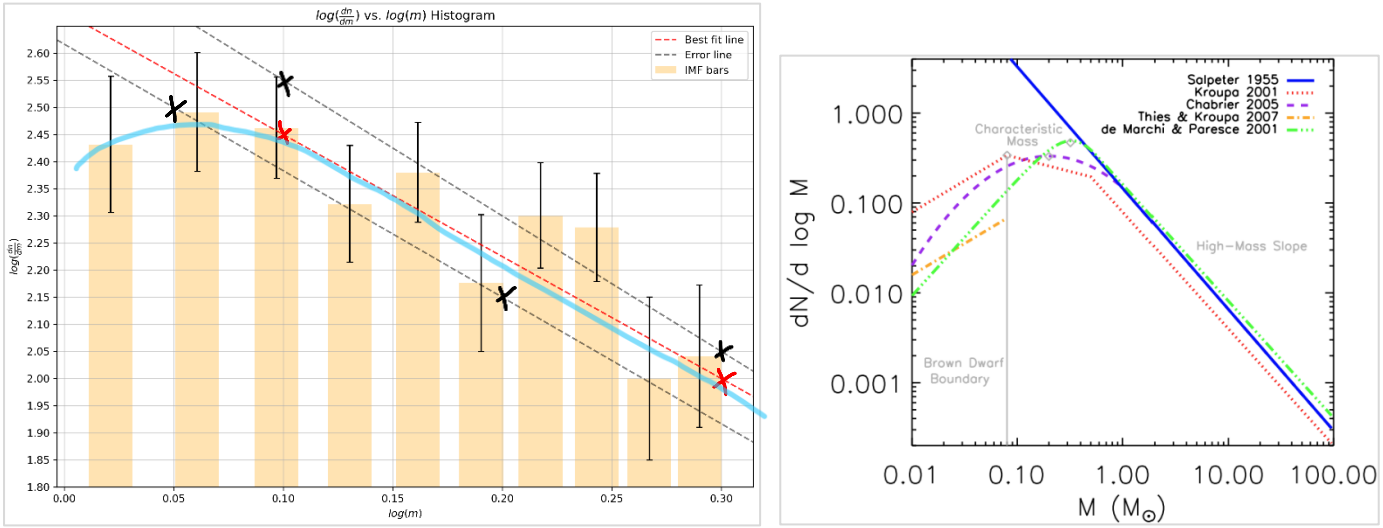

Figure 3, 4: Comparison of the experimental IMF histogram with the literature. Fig. 3 (on the left) shows the IMF plot based on the observed data. We can see a Salpeter-like downward slope after reaching a maximum at around log (m) = 0.06. The slope of the solid blue line in Fig. 4 (on the right) where the IMFs asymptote to depicts Salpeter's well-known value of α = 2.35 (Offner et al., 2014).

The error bars on the $\log\left(\frac{dn}{dm}\right)$ value is propagated by the formula:

$$\delta\left[\log\left(\frac{dn}{dm}\right)\right] = \frac{1}{\left(\frac{dn}{dm}\right)\cdot \ln(10)}\delta\left(\frac{dn}{dm}\right), \qquad where\ \delta\left(\frac{dn}{dm}\right) = \frac{\delta(dn)}{dm} \ldots (5)$$

D. Assess, interpret the α value & discussion

By fitting a straight (red dashed) line where the curve asymptotes to in **Fig**. 3, the α value (i.e. the slope) is found to be:

$$\alpha = -\frac{y_2 - y_1}{x_2 - x_1} = -\frac{2.45 - 2.00}{0.30 - 0.10} = 2.25 \ldots (6)$$

To evaluate the uncertainty, we approximate the slopes of two lines that enclose the red dashed line, and the uncertainty would be the central difference between these two slopes. Therefore:

$$\delta\alpha = \frac{1}{2}\left(\left|\frac{2.55 - 2.05}{0.10 - 0.30}\right| + \left|\left(\frac{2.15 - 2.50}{0.20 - 0.05}\right)\right|\right) - \alpha = \frac{1}{2}|4.83| - (2.25) = 0.17 \ldots (7)$$

Finally, combining **Eq**. (6) and (7), we get:

$$\alpha = 2.25 \pm 0.17 \ldots (8)$$

, which is close to Salpeter's original value of $\alpha = 2.35$ within the error range.

If brown dwarfs (BDs) and stars contribute equally to the overall galactic mass, by integrating the IMF over the brown dwarf and star mass ranges:

$$\int_{0.013}^{0.08} m\xi(m)\,dm = \int_{0.08}^{\infty} m\xi(m)\,dm \rightarrow \int_{0.013}^{0.08} m \times m^{-\alpha}\,dm = \int_{0.08}^{\infty} m \times m^{-\alpha}\,dm \ldots (9)$$

After simplifying the terms and integration, we get:

$$\frac{1}{2-\alpha}[m^{2-\alpha}]_{0.013}^{0.08} = \frac{1}{2-\alpha}[m^{2-\alpha}]_{0.08}^{+\infty}$$

$$(0.08)^{2-\alpha} - (0.013)^{2-\alpha} = \lim_{m\to\infty} m^{2-\alpha} - (0.08)^{2-\alpha} \ldots (10)$$

The limit term involving infinity in **Eq**. (10) has three possible cases:

$$\lim_{m\to+\infty} m^{2-\alpha} = \begin{cases} +\infty & (when\ \alpha < 2) \\ 1 & (when\ \alpha = 2) \\ 0 & (when\ \alpha > 2) \end{cases}$$

Assuming $\alpha \geq 2$, we get:

$$2(0.08)^{2-\alpha} = (0.013)^{2-\alpha}$$

By taking the logarithm, we find that:

$$\alpha = \frac{\log 2 + 2\log(0.08) - 2\log(0.013)}{\log(0.08) - \log(0.013)} \approx 2.38$$

, which is higher than both the measured and the standard Salpeter's value.

There is evidence suggesting that due to different environments in the star formation process, the power law $\xi(m) \propto m^{-2.35}$ no longer holds and the value of α changes at two critical masses, 0.08 and 0.5 M_{Sun}. The Salpeter value of α is only applicable to high-mass stars, around 0.5 M_{Sun} to 100 M_{Sun} (Kroupa, 2001). Sub-stellar masses (BDs) have an average estimate of $\alpha = 0.3 \pm 0.7$. The shallower slope implies that the calculation of α in **Eq**. (9) is an overestimate since BDs in reality do not contribute significantly to the total galactic mass.

Different star formation conditions cause the difference in the observed α value between low and high-mass stars, which are useful for astronomers to better understand the star formation process. Fragmentations are more common in regions of denser molecular clouds and gas, creating more low-mass stars. Also, the impact of the feedback mechanism on the low and high-mass star formation regions is not the same. High-mass stars cause stronger stellar winds and more intense radiation which can obstruct further star formation (Bate, 2009), while the thermal equilibrium process affects low-mass stars more, having more low-mass stars in the region than the Salpeter's value would predict. These lead to different slopes observed in low and high-mass star regions in the IMF.

The results from different astronomer's simulations generally agree with Salpeter's value within the mass range of 1 to 2 M_{Sun}. In **Fig**. 5, we can see that the function has a flatter slope when the stellar mass is below around 0.5 M_{Sun}, and then it starts to show a steeper Salpeter-type slope, aligning with Salpeter's prediction.

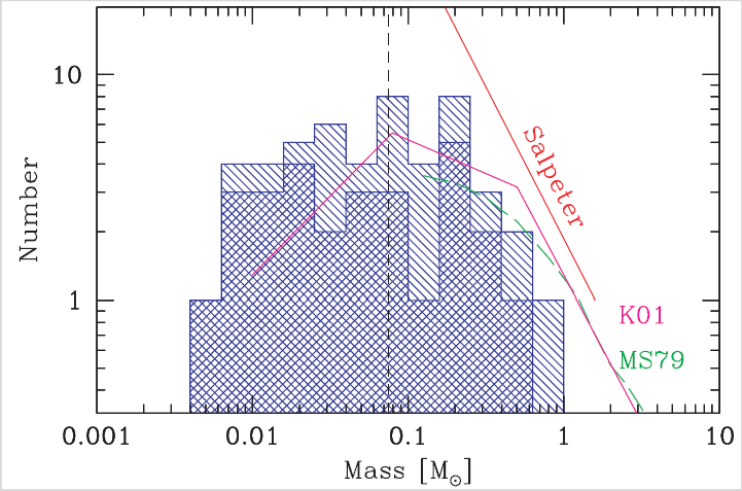

Figure 5: Comparison of the computer simulation with the characteristic Salpeter slope. All the objects reside in the single-shaded region, only those that finished the accretion process sit in the double-shaded region (Bate et al., 2003).

IV. Conclusions

The IMF helps astrophysicists to better understand the distribution of stars in the star formation process. We calculated the α value for the M35 cluster for MS stars with mass ranging from 1 to 2 M_{Sun} and compared it to Salpeter's well-known value of $\alpha = 2.35$. Computer simulations using Salpeter's prediction generally align with stellar masses from around 0.5 to 100 M_{Sun}. Yet, Salpeter's value does not apply to stars across all mass ranges. We discussed how the differences in the fragmentation process and the impact of feedback mechanism on low and high-mass star formation regions account for the different α values observed in low-mass stars.

References

Salpeter, E.E., 1955. The luminosity function and stellar evolution. *Astrophysical Journal, vol. 121, p. 161*, *121*, p.161.

Offner, S.S., Clark, P.C., Hennebelle, P., Bastian, N., Bate, M.R., Hopkins, P.F., Moraux, E. and Whitworth, A.P., 2014. The origin and universality of the stellar initial mass function. *Protostars and Planets VI*, *53*.

Kroupa, P., 2001. On the variation of the initial mass function. *Monthly Notices of the Royal Astronomical Society*, *322*(2), pp.231-246.

Bate, M.R., 2009. The importance of radiative feedback for the stellar initial mass function. *Monthly Notices of the Royal Astronomical Society*, *392*(4), pp.1363-1380.

Bate, M.R., Bonnell, I.A. and Bromm, V., 2003. The formation of a star cluster: predicting the properties of stars and brown dwarfs. *Monthly Notices of the Royal Astronomical Society*, *339*(3), pp.577-599.

Appendix – Images of the observed cluster (M35) and its offset field

1. M35_V_120s_B4_T9_108080.fit

Figure 3: Image of the cluster field M35 in V-band from the automated plan.

2. M35_B_180s_B4_T9_108091.fit

Figure 4: : Image of the cluster field M35 in B-band from the automated plan.

3. M35_offset_field_V_120s_B4_T9_108101.fit

Figure 5: Image of the offset field for M35 in V-band from the automated plan.

4. M35_offset_field_B_180s_B4_T9_108113.fit

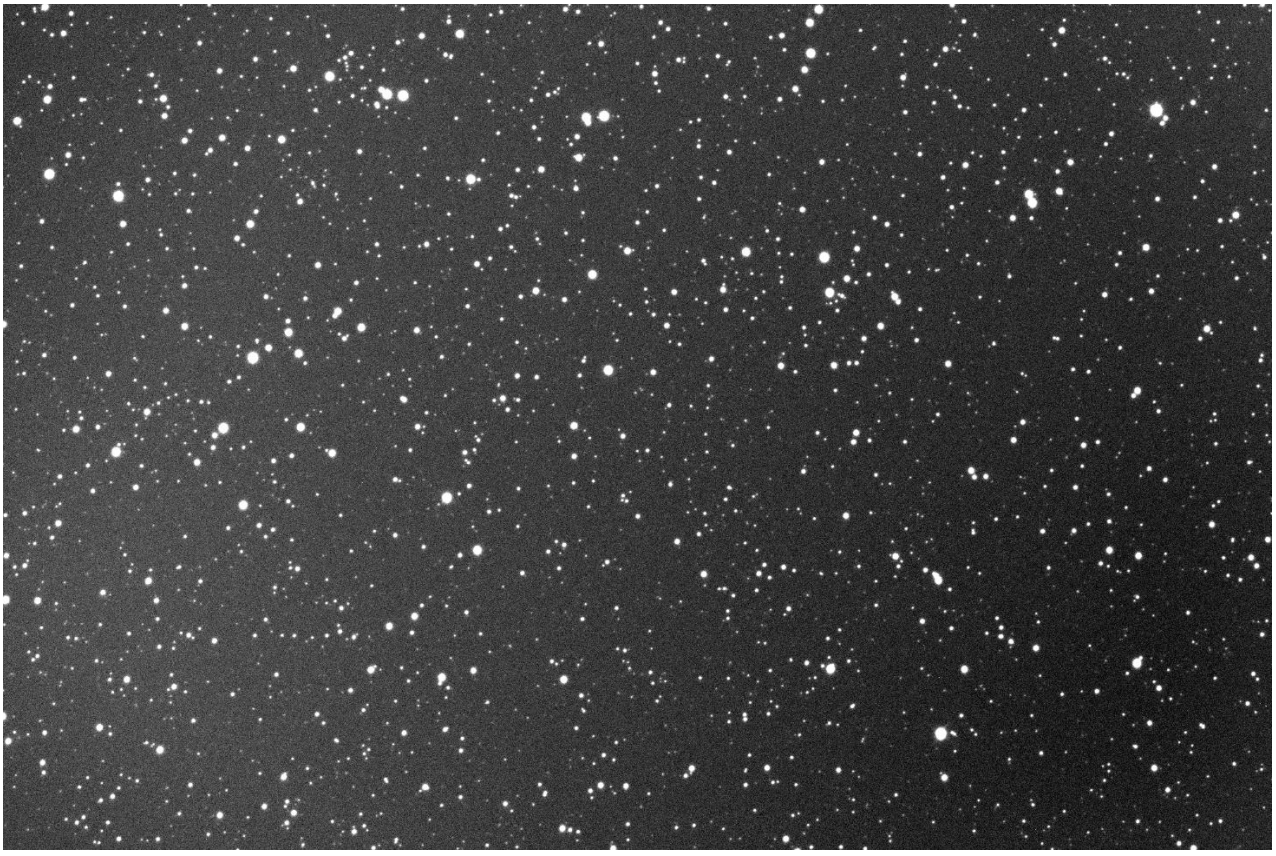

Figure 6: Image of the offset field for M35 in B-band from the automated plan.